Egypt. J. Chem. **Vol. 64,** No. 2 pp. 661 - 672 (2021)

Egyptian Journal of Chemistry

http://ejchem.journals.ekb.eg/

Green Synthesis of Zinc Oxide Nanoparticles Using Portulaca *oleracea (*Regla Seeds) Extract and Its Biomedical Applications

Hend Y. G. Mohamed[a], Eman H. Ismail[a], Mahmoud M. Elaasser [b], Mostafa M.H. Khalil[a,*]

[a] *Chemistry Department, Faculty of Science, Ain Shams University, Abbassia, 11566, Cairo, Egypt*

[b]*The Regional Center for Mycology and Biotechnology, Al-Azhar University, Cairo, Egypt*

Abstract

In the present study, the biosynthesis of ZnONPs utilizing *Portulaca oleracea* seeds aqueous extract has been reported. The reported method is a green, plant-extract mediated and low-cost approach that is capable of synthesizing ZnONPs at pH 7 with heating at 60 ºC for one hour. To demonstrate the efficiency of the capping bioorganic molecules on ZnO nanoparticles, a part of the product was dried at 60 ºC (denoted ZnO-60) and the other part was annealed at 500 ºC (denoted ZnO-500). Both synthesized ZnONPs was crystalline in nature and hexagonal in shape with an average size of 14 nm and 34.5 nm for ZnO-60 and ZnO-500, respectively, as evidenced by XRD and TEM analysis. The synthesized nanoparticles showed high antioxidant, good antibacterial activity, which has inhibited the growth of Helicobacter pylori (ATCC 700392) and Methicillin-Resistant Staphylococcus aureus bacteria and anticancer activity for HCT-116 cells with a higher efficiency of ZnO-60 than ZnO-500

Keywords: Biosynthesis; Zinc oxide nanoparticles; *Portulaca oleracea* extract; antimicrobial; antioxidant; antitumor.

1. Introduction

Zinc oxide is a non-toxic and multifunctional inorganic material that has vast area of applications in different fields [1]. Zinc oxide with a broad bandgap of (~3.3 eV), exhibits semiconducting properties, having good piezoelectric properties and optoelectronics. Due to its unique physical and chemical properties, it is utilized in many industries such as sunscreen and burning ointments, antibacterial treatments, lotions, self-cleaning coating material on ceramic and glass surfaces, diodes, transistors manufacturing, and display screens. It is used as Uv-absorbent, dental cement manufacturing, gas sensors in the varistors, fire extinguishers [2-4], and solar cells [5]. There are many chemical and physical methods for zinc oxide nanoparticles (ZnONPs) production [6, 7]. Synthesis of nanoparticles using chemical and physical methods has a lot of disadvantages, including the use of hazardous chemicals and toxic solvents, which is non-eco-friendly [8]. Green synthesis of metal oxide nanoparticles using plant extracts has been attracted great consideration of many researchers because of the advantages it has over the chemical and physical methods. During the synthesis of metal oxide nanoparticles using green methods, the extract of plants plays an active role in the synthesis process because it contains biomolecules that act as reducing agents that perform redox reactions by transferring electrons to metal ions producing metallic nanoparticles, and as a capping agent to prevent agglomeration. There are much previous research used extracts of different parts of a plant for the synthesis of ZnONPs, such as *Aloe vera* leaf extracts [9, 10], *Physalis alkekengi* L. seed extract [11], *Hibiscus rosasinensis* [12], the leaf extract of *Camellia sinensis* [13], the aqueous extract of seeds of five divergent vegetables belonging to the family *Brassicaceae* [14], *Rosa canina* fruit extract [15], *Citrus aurantifolia* (lemon) peel extract [16], *Selaginella convolute* leaf extract [17], *Morus nigra* leaf extract [18], *Dittrichia graveolens* aqueous extract [19] and *Rehmanniae Radix* [20]. All the previous researches confirmed that green synthesized ZnONPs have a great antibacterial activity against a broad spectrum of Gram(+) and Gram(-) bacteria, photocatalytic and anticancer activity, therefore it is

*Corresponding author e-mail: khalil62@yahoo.com, mostafa_khalil@sci.asu.edu.eg.; (Mostafa M.H. Khalil).
Receive Date: 08 October 2020, Revise Date: 17 October 2020, Accept Date: 25 October 2020
DOI: 10.21608/EJCHEM.2020.45592.2930

involved in the manufacture of many drugs in addition to it occupies a distinguished position in various scientific researches.

Portulaca oleracea L. (purslane) grows widely in diverse areas of the world including Egypt (known as Regla). The leaves and seeds of *Portulaca oleracea L.* have many therapeutic applications such as a diuretic, antipyretic, antiasthma, anti-inflammatory, and anti-tussive uses [21]. Also, various studies have verified diverse pharmacological effects of *Portulaca oleracea L.* in conjunction with hypoglycaemic [22], hypocholesterolemic [23], treatment of type-2 diabetes mellitus [24], antioxidant [25], and against influenza A viruses [26]. The purslane has different biocompounds, in addition to alkaloids, omega-3 fatty acids (linolenic acid, α-linolenic acid), coumarins, flavonoids, phenolic compounds (protocatechuic and *p*-hydroxybenzoic acids) [27], polysaccharide, vitamins, and dietary minerals such as calcium, magnesium, potassium, iron, and oxalate [28, 29]. It was found that the seeds of *Portulaca oleracea* (Regla seeds) are more effective than the other parts [30]. In addition, the *Portulaca oleracea* seeds contain about 17.4% concentration of a non-volatile oil and containing α-sitosterol [31].

Green synthesis of ZnO nanoparticles was widely studied before, but to our best knowledge, there are no reports on its green synthesis using *Portulaca oleracea* seeds (Regla seeds) extract. In the present study, the biological synthesis of ZnONPs using Regla seeds aqueous extract has been investigated. The bio-molecules that exist in the seeds extract can act as reducing and/or capping agents for stabilization of the NPs formed. Furthermore, the extract of *Portulaca oleracea* seeds as a capping agent surrounds the ZnO nanoparticles can enhance the antimicrobial properties, stability, and biocompatibility of the nanoparticles [32, 33]. ZnONPs were synthesized using *Portulaca oleracea* seeds at pH 7 and 60 ^{0}C, then a part of the product was dried at 60 ^{0}C to keep the extract compounds on the ZnO surface and the other part was heated to 500 ^{0}C to get rid of the capping extract and obtain pure ZnONPs. As known, *S. aureus* is from the well-established organisms that is difficult to treat because of resistance to some antibiotics; the resistant bacteria to methicillin and its derivatives (Methicillin-resistant *Staphylococcus aureus*, MRSA) is well-thought as the most aggressive cause of nosocomial infections. MRSA infections are very demanding to treat because of bacterial resistance to most of the clinically functional antibiotics [34]. It was found that the seeds extracts of *P. oleracea* had only antibacterial activities toward normal *S. aureus* strains but not against MRSA isolates [34]. Owing to an increase in antibiotic resistance, using metal oxides nanoparticles can be a competent option. The effect of using capping ZnONPs (ZnO-60) and naked ZnONPs (ZnO-500) on the antibacterial activity against a Gram (+ve) bacterium (Methicillin-resistant *S. aureus*) and a Gram (-ve) bacterium (*H. pylori*) was evaluated. The antioxidant and the cancer activity of the green synthesized ZnONPs using *P. oleracea* aqueous extract were also evaluated.

2. Materials and Methods

2.1. Materials: Zinc nitrate hexahydrate ($Zn(NO_3)_2.6H_2O$, 99.9%) was purchased from Aldrich. *Portulaca oleracea* seeds were purchased from standard vend.

2.2. Preparation of Portulaca oleracea seed extract: The *Portulaca oleracea extract* extract (2.5 % w/v) was prepared by adding 2.5 g of dried seeds to 100mL deionized water and boiling the solution for 20 min. Then the extract was cooled followed by filtration through Whatman paper No. 1 and the solution was completed to 100 ml with de-ionized water. For all experiments, the extract was freshly prepared.

2.3. Synthesis of ZnONPs using Regla seeds aqueous extract:

A 2.5 x10^{-2} M stock solution of zinc nitrate hexahydrate was prepared by weighing out 0.75g of zinc nitrate hexahydrate and dissolving in 100 mL deionized water. To synthesize ZnO nanoparticles, a certain volume of *Portulaca oleracea* seeds extract was added to a certain volume of $Zn(NO_3)_2.6H_2O$ at room temperature and then completed to 10 ml with deionized water. The optimization study was carried out considering different parameters such as zinc nitrate concentration ($2.5x10^{-3}$-$1x10^{-2}$ M), the quantity of the extract (1-3 ml), reaction time (5-60 min.), pH (3-11), and temperature (20-80 ^{0}C). The formation process of ZnO nanoparticles was followed by the Uv-Vis spectrophotometer. Using the optimum conditions, the ZnONPs prepared by adding 15ml of the extract dropwise to 50 ml zinc nitrate (2.5 x10^{-2} M) followed by heating the solution at 60 ^{0}C for 1h till the color of the extract disappeared and white jelly precipitate are obtained. The product was then divided into two parts: one part of the product was dried in the oven at 60 ^{0}C (denoted as ZnO-60) and the other part of the product was taken and put into a crucible and was reserved in the furnace for calcination at 500 °C for 2 h (denoted as ZnO-500). After calcination, zinc oxide nanoparticles were obtained in white colored powder.

2.4. Characterization of ZnONPs

The absorption spectra of ZnONPs was measured on Shimadzu model 2600 Uv-vis spectrophotometer at

wavelengths between 200-600 nm using 10 mm optical path length quartz cuvettes. The size and morphology of the synthesized ZnO nanoparticles were examined using TEM images obtained on a JEOL-1200JEM and HR-TEM, model JEOL-JEM 2100, Japan. Transmission electron microscopy samples of ZnONPs were conducted by placing a drop of the suspension of the bio-synthesized ZnONPs onto carbon-coated copper grids and allowing the solvent to evaporate in air. XRD measurement of the ZnONPs was done on a Shimadzu XRD-6000 diffractometer working at a current of 20 mA and a voltage of 40 kV with Cu Kα radiation (λ= 1.54 Å). Nicolet 6700 FTIR spectrometer was used to obtain FTIR spectra at room temperature. The dried ZnONPs samples are mixed with KBr in the form of a round disk and it was measured in the range of 400-4000 cm^{-1}. Similarly, FTIR of Regla seeds was obtained by grinding dried seeds with KBr.

2.5. Anti-MRSA Activity

A MRSA clinical isolate was kindly obtained from the Regional Center for Mycology and Biotechnology (RCMB) culture collection at Al-Azhar University, Cairo, Egypt. The activity of synthesized ZnONPs against MRSA was investigated using the well diffusion agar method [35, 36]. The MRSA isolate grown in Muller Hinton media till counting 10^8 cells/ml was then inoculated on agar plates. One hundred microliter of each ZnONPs was added at 10 mg/mL to each well (6 mm diameter holes cut in the agar gel), then incubated at 37°C for 24 h. After incubation, the inhibition zone diameters were calculated. DMSO that used for dissolving ZnONPs was also tested as solvent control showing no inhibition zones. Positive control was also performed using norfloxacin as a standard antibiotic. The minimum inhibitory concentration (MIC) was then measured by the same methods using different concentrations from ZnONPs to determine the minimum inhibitory concentration **[36]**.

2.6. Determination of Anti-H. pylori Activity

The activities of the tested ZnONPs against *Helicobacter pylori* (ATCC 700392) were performed as described previously [37] using broth microdilution method. The tested serial dilutions of the ZnONPs (ranged from 10000 to 10 µg/mL) were added in a 96-well microtiter plate having 100 µl of freshly prepared Mueller-Hinton medium with 10% defibrinated sheep blood (Lonza, Belgium). A 100 µl liquid culture from 3-days-old *H. pylori* was inoculated into each well to provide a final conc. of 1 x 10^6 colony forming units (CFU/well). The microtiter plates were then incubated for 3 days at 37°C in a microaerophilic atmosphere (5% O_2, 10% CO_2 and 95% relative humidity) in a double-gas CO_2 incubator (ShelLab, USA). Metronidazole antibiotic was tested as positive control. After end of incubation, lowest concentration that showed complete growth inhibition was recognized as the MIC of tested sample **[38]**.

2.7. Antitumor activity assay:

HCT-116 (human colorectal carcinoma cell line) cells were purchased from American Type Culture Collection (ATCC, Rockville, MD). The cells were grown on RPMI-1640 medium supplemented with 50µg/ml gentamycin, 10% heat-inactivated fetal calf serum and 1% L-glutamine in a 5% CO_2 incubator (ShelLab 2406, USA) at 37ºC.

In antitumor assay, the HCT-116 cells were added at concentration $5x10^4$ cell/well in RPMI-1640 medium, then incubated at 37ºC for 24 h in Corning® 96-well tissue culture plates. Different concentrations from ZnONPs were then added (started from 500 to 1µg/ml; three replicates each). After incubating for 48 h, the numbers of viable cells were determined by the MTT assay **[36, 39]**. After plotting the dose-response curve, the IC_{50} (concentration that decreases the cells by 50 %) was calculated.

2.8. DPPH assay

The DPPH free radical scavenging abilities of biologically synthesized ZnONPs were assayed as described by Puvanendran et al. [40]. Briefly, 40 µL nanoparticles solution was added to 3 mL of methanolic DPPH solution (0.004% w/v) and vortexed for 30 s. UV-visible spectrophotometer (Milton Roy, Spectronic 1201) was used to record the absorbance at 515 nm. Decreasing absorbance of the DPPH solution with or without the sample was measured after 16 min. Ascorbic acid was tested as positive control. Three replicates were performed for all samples and controls. The DPPH radical scavenging percentage was calculated from the following equation:

$$\text{DPPH radical scavenging } \% = \left[\frac{Ac-Aa}{Ac}\right] x100$$

where Ac = absorbance of control without sample at 0 min, and A_a = absorbance of reaction solution at 16 min. After plotting the dose-response curve, the IC_{50} (concentration that decreases absorbance of DPPH solution by 50 %) was calculated.

2.9.Trypsin inhibition study:

The enzymatic inhibitory activity of the tested ZnONPs towards trypsin was evaluated with *N*-α-benzoyl-L-arginine p-nitroanilide (BAPNA) as the substrate as previously described **[41]**. The tested nanoparticle(s) were dispersed in Tris-buffer (1 ml, 0.05M, pH 8.2) containing $CaCl_2$ (0.02 M) to reach a final concentration of 0.1% w/v. After adding 30U of trypsin solution (0.3 ml in 10mM HCl), the mixture was incubated at 37°C. Thereafter, 2.1 ml of the BAPNA solution (20mM in DMF) was added and

incubation continued for 15 min at 37°C. After stopping the enzymatic action with 1% trichloroactetic acid solution, the nitroaniline formed (Yellow color) was analyzed by measuring the absorbance at 405 nm using a UV/visible spectrometer (Milton Roy, Spectronic 1201). Controls without the tested nanoparticles were also performed. Three replicates were performed for all samples and controls.

Trypsin Inhibition Activity (%) = $(\frac{AC-AT}{AC})x\ 100$
Where *A*C = Absorbance of the control and *A*T = absorbance of the test sample.

3. Results and Discussion

3.1. Uv–Visible spectroscopy

The molar ratio of Zn(II) : extract is an important factor in the synthesis of ZnONPs. Preliminary experiments are performed by adding different extract concentrations on $Zn(NO_3)_2.6H_2O$ ($2.5x10^{-5}$M) and heating at 60 ^{0}C for 30 min, which led to an increase in the absorbance at 279 nm which is the same absorption peak for the extract without any shift in the absorption peak. On the other hand, using a constant volume of Regla seeds extract (2ml, 2.5%w/v) and different volume of $Zn(NO_3)_2.6H_2O$ (1, 2,4,6 and 8 ml, of $2.5\ x10^{-2}$ M) with heating to 60 ^{0}C for 30 min, a red shift in the band from 279 nm to 303 nm (Fig. 1b) was observed without any precipitate, indicating the formation of Zn complex with the biomolecules such as polyphenoles, flavonoids, and fatty acids present in the extract. Previous studies suggest that the plant extract contains compounds that react with zinc salt to form Zn(II)-coordinated complexes that decompose thermally to form ZnONPs [42, 43, 44, 45]. However, another mechanism for biosynthesized ZnONPs proposed by Singh et al. (2018) [46] where the biomolecules reduce Zn(II) ions into metallic zinc, then the metallic zinc reacts with oxygen to form ZnONPs stabilized by the extract to prevent agglomeration.

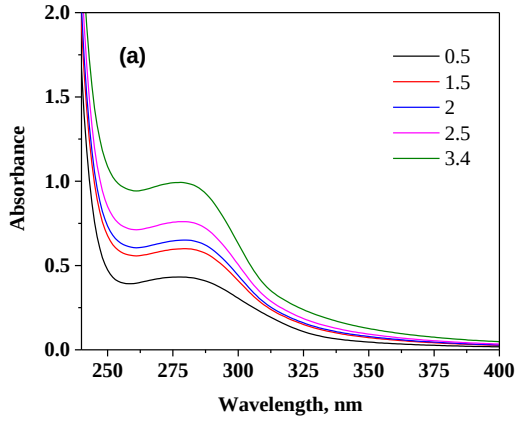

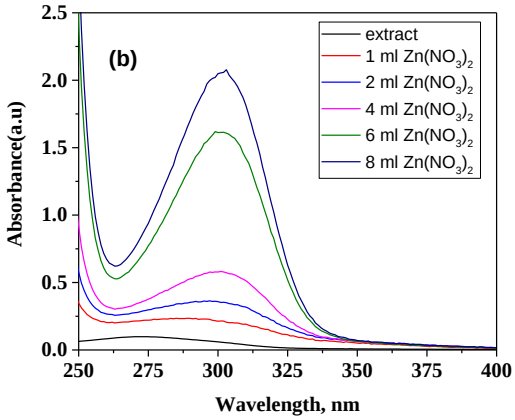

Figure 1. a) Effect of *portulaca oleracea* (regla seeds) extract concentration on ZnO formation; $(ZnNO_3)_2$, $2.5x10^{-5}$M, b) using constant extract concentration (2 ml, 2.5%) with different ; $(ZnNO_3)_2$ concentrations

3.2. Effect of *portulaca oleracea* (regla seeds) extract pH:

The pH of the extract used in the biosynthesis of ZnONPs is a crucial factor affecting the size, shape, and composition of the nanoparticles. With the help of Uv-vis spectroscopy, the impact of Regla seeds extract pH on the biosynthesis of ZnONPs is studied. The Regla seed aqueous extract pH was 4 without any additions. Using zinc nitrate (8ml, final concentration $1x10^{-2}$M) and Regla seed extract 2 mL at pH 4 (with heating to 60 ^{0}C), a broad absorption band centered at 305 nm is observed (Fig. 4a). Adding HCl (0.05M) to adjust pH at 3 and 2, lead to a decrease in the absorption spectra without any shift in the absorption maximum. On the other hand, increasing pH to 7 with 0.05M NaOH, the absorption spectrum exhibit a shift to 340 nm indicating the formation of ZnONPs. The SPR band of ZnONPs decreases with increasing the pH of Regla seed extract to pH=11 accompanied by a red shift in the SPR band to 355 nm indicating the formation of smaller size uniform nanoparticles. Ameen et al. (2013) [47] reported that the appearance of an SPR band in the region 300–400 nm confirmed the formation of ZnONPs. This shorter wavelength indicates that the particles have smaller sizes (see below). In this study, we prefer using the neutral pH of Regla seed extract at (pH=7) as this is better for biological applications.

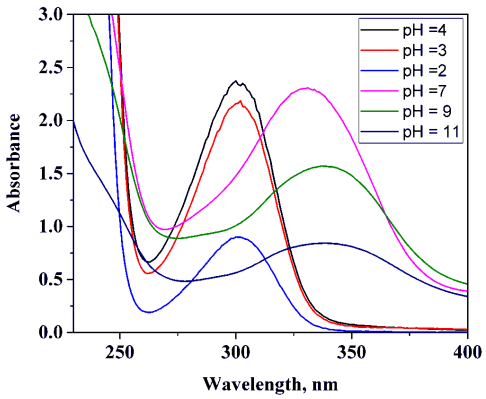

Figure 2. Effect of pH on the formation of ZnONPs

3.3. Characterization of ZnONPs

Fig.3 shows the XRD pattern of the biosynthesized ZnO-NPs. The distinct diffraction peaks at 2θ =31.717°, 34.484°, 36.245°, 47.585°, 56.705°, 62.826°, 66.580°, 68.025°, and 69.039° were assigned to (100), (002), (101), (102), (110), (103), (200), (112), and (201) planes, respectively. All the relative peaks of the biosynthesized ZnO-NPs were matched with the (JCPDS) card number 00-065-0725 in terms of intensities and positions. All the peaks recorded in Fig. 3 were well indexed to the hexagonal phase of ZnO and the nanopowder was shown to be highly crystallized owing to the narrow and sharp peaks. The high intensity at the peak of (101) was an indication of a preferred orientation of the crystallites. No impurities, such as $Zn(NO_3)_2$, $Zn(OH)_2$, or other organic compounds can be detected from the XRD patterns of the ZnO-500 sample, whereas, it can be observed that, for ZnO-60, there is a broad peak centered at about $2\theta = 24^0$ could be assigned to the crystallization of the organic constituent on the surface of the ZnONPs. The crystallite size of the particles (D) calculated using the full width at half-maximum (FWHM) of the diffraction peak according to the Scherrer equation, $D=K*\lambda/\beta*\cos\theta$ Where λ is the wavelength of the incident X-ray beam; θ is the Bragg's diffraction angle; β the full width at half-maximum (FWHM) in radian and the dimensionless shape factor (K) has a value of 0. 9. The XRD patterns of ZnO-60 showed more broadening of the peaks compared to ZnO-500 patterns due to the particle size effects [48]. The values were found to be 31.18 nm (Zn-500) and 17.2 nm for ZnO-60 (Fig 3), as confirmed by TEM micrographs.

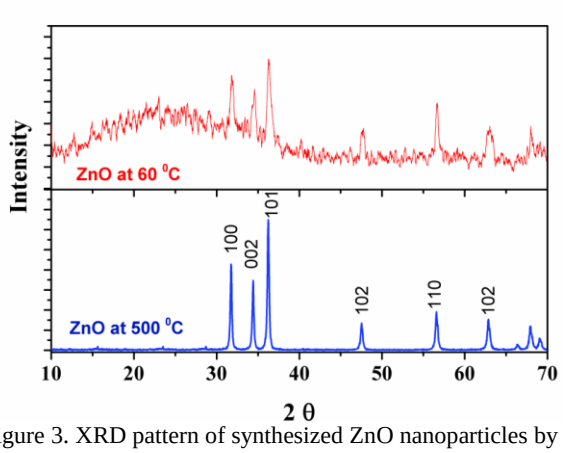

Figure 3. XRD pattern of synthesized ZnO nanoparticles by *portulaca oleracea* (regla seeds) extract

The TEM image of ZnONPs was shown in Fig. 4. For the sample dried at 60°C, one can observe a series of small particles with size ranging from 10 to 18 nm with a certain degree of short-range atomic ordering are observed. On the other hand, the annealed sample at 500 °C showed highly crystalline nanoparticles with edged interfaces with their average spherical equivalent diameter ranges from 22 to 45 nm. This larger size of annealed sample indicated that annealing and evaporation of the organic biomolecules lead to some agglomeration and crystallite arrangement. Also, a series of small rods with the basal and longitudinal sizes of 18–55 nm as well as cubic structures can be observed. The annealed ZnO-500 NPs were showed unequal surface morphology with larger size than ZnO-60 NPs; the particle size measured from the TEM images were in agreement with the sizes obtained from X-ray of 31.18 nm (Zn-500) and 17.2 nm for ZnO-60.

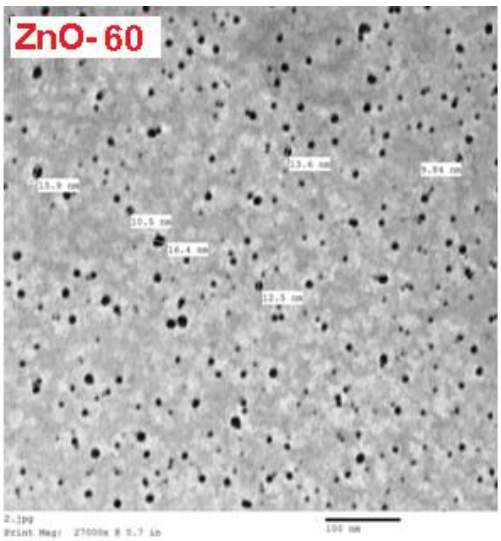

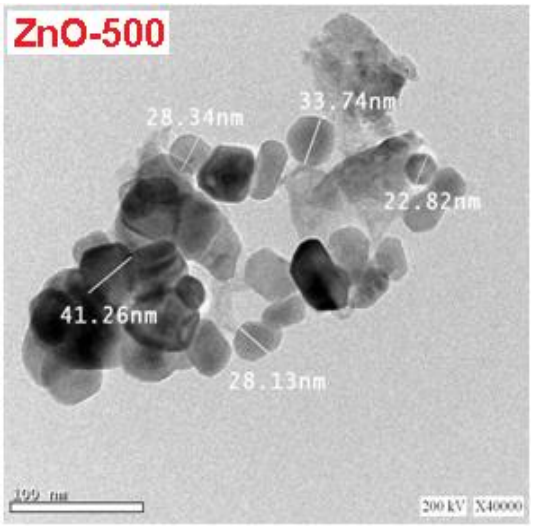

Figure 4. TEM images of ZnONPs dried at 60 ^{0}C and annealed at 500 ^{0}C.

3.4. Fourier Transform Infrared Spectroscopy (FT-IR) analysis

The FTIR spectrum of Regla seeds, Fig.5, exhibited various peaks in solids or after aqueous extract. The FTIR peaks of the solid Regla seeds showed bands at 3259 cm^{-1} and 3011 cm^{-1} which were assigned to stretching vibrations of OH and NH groups **[49, 50],** and the strong peaks at ~ 3011, 2923 and 2853 cm^{-1} were assigned to -CH stretching showing the presence of CH_2, CH_3 groups in the fatty acids. The strong band at 1744 cm^{-1} was assigned to –C=O group of ester or carboxylic acid. The band at 1654 cm^{-1} could be assigned to the C=O of the amide group stretching vibration. The bands at 1510, 1460and 1376 cm^{-1} are due to C=C (aromatic ring) and C-C stretching vibrations. The bands at 1155 and 1017 are attributed to C-N and C-O stretching vibrations. To get a closer view, the ATR-FTIR was measured for the water extract, As can be seen in Fig, 5, many peaks of the seeds are absent indicating that not all the organic compounds could be obtained in the aqueous extract. The strong peak at 3443 and a shoulder 3174 cm^{-1} due to OH and NH groups present in the aqueous extract. The band at 1645 cm^{-1} attributed to C=O of the amide group and could be related to flavonoid and amino acids [**51**]. The FTIR of ZnO-60 showed peaks at 3368 cm-1 (due to OH stretching); shoulder at 1654 cm^{1} (aromatic C=C stretching), and 1017 cm^{-1} due to –C-O stretching vibrations of the phenolic groups present in the plant extract. Also, aromatic C-H out of a plane at 716 cm^{-1} in the seeds and at 836 cm^{-1} for ZnO-60 was detected. Furthermore, the peaks under 500 cm^{-1} (459 cm^{-1}), Figure 5, due to the Zn-O bonds vibration mode supporting the formation and purity of the ZnONPs structure [52]. For ZnO-500, this band was observed at lower than 400 cm^{-1}. This shift can be correlated to a change in the lattice parameters of the ZnONPs with an increase in the annealing temperature. Zak et al. [**53**] observed Zn-O vibration bands at 370-375 cm^{-1} when annealing temperature increased from 600-750 ^{0}C.

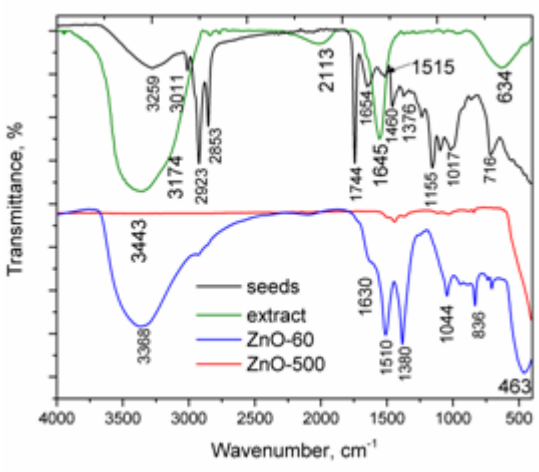

Figure 5 FTIR spectra of regal seeds, extract, ZnO-60 and ZnO-500 nanoparticles

3.5. Antibacterial activity of ZnONPs

The antibacterial activity of the synthesized ZnONPs was investigated against two potentially pathogenic microorganisms: one gram-positive bacterium (Methicillin-resistant *S. aureus*) and one gram-negative bacterium (*H. pylori*).

The inhibitory effect of the synthesized zinc nanoparticles on *Helicobacter pylori* (ATCC 700392) compared with a regular antibiotic (Metronidazole) was used as a positive control (1000 µg/mL). The tested concentration from zinc nanoparticles was 2000 µg/mL. ZnO-60, ZnO-500, and the extract exhibited inhibition zone diameter of 14.2, 10.9, and 6.8 mm against *H. pylori* strain by the well-diffusion assay when compared with a standard antibiotic (Metronidazole) (19.5 mm) as shown in Fig 6a.

The MIC values demonstrated that ZnO-60 nanoparticles showing to be more potent (MIC: 0.75 mg/ml) than ZnO-500 nanoparticles (MIC: 2 mg/ml). Additionally, Fig 6 showed that the antibacterial activity of the synthesized zinc nanoparticles was also investigated against gram-positive bacteria, Methicillin-Resistant *Staphylococcus aureus* (MRSA) using the agar well diffusion method with standard antibiotic (Norfloxacin) as a positive control (Fig. 6a). The zone of inhibition diameter of 31 mm was observed by ZnO-60 nanoparticles against MRSA strain revealed significant difference when compared with those of Norfloxacin (standard), while the least activity was seen ZnO-500 nanoparticles (Figure 6a). On the other hand, the measured MIC values for ZnO-60 nanoparticles were also more

potent (MIC: 1 mg/ml) than ZnO-500 nanoparticles (MIC: 5 mg/ml) when tested against MRSA, Fig. 6b. The *P. oleracea* extract was reported to have a potent activity toward Gram-positive bacteria, *Bacillus subtilis*, and *S. aureus*, and the extract was found to be only active toward one Gram-negative bacterium, i.e. *P. aeruginosa* [**54]**. Due to its low toxicity to mammalian cells [**55,56, 57**] high influence against antibiotic-resistant strains, and low cost, ZnO seems to be more promising for clinical applications.

The mode of actions between ZnO-NPs as drug and bacterium remains not clear. Some reports suggested that the occurrence of ROS may affect only cell death in bacterial biofilms irregularly and may increase development of biofilm [**58**]. Interaction of metal and metal oxide nanoparticles with various cell models and their cell impacts have been reviewed [**59**] and exhibited that the cooperation of ROS through the interaction of the nanoparticles with different cell models. Moreover, some studies reviewed the bacterial ability to use excess ROS formed into many respiratory and metabolic pathways [**60, 61**]. Kadiyala, et al. studied the antibacterial activity of ZnONPs against methicillin-resistant *Staphylococcus aureus* (MRSA) and concluded that small role of ROS production and the large role of alterations in carbohydrate metabolism and bioenergetics [**62**].

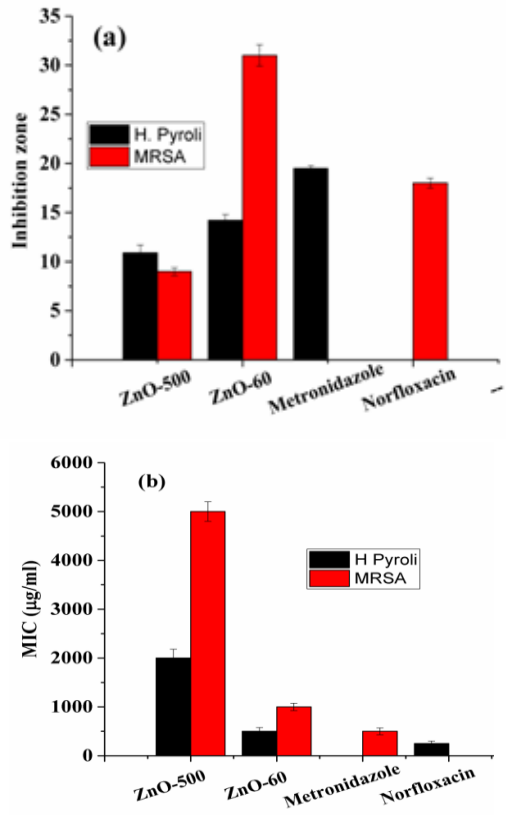

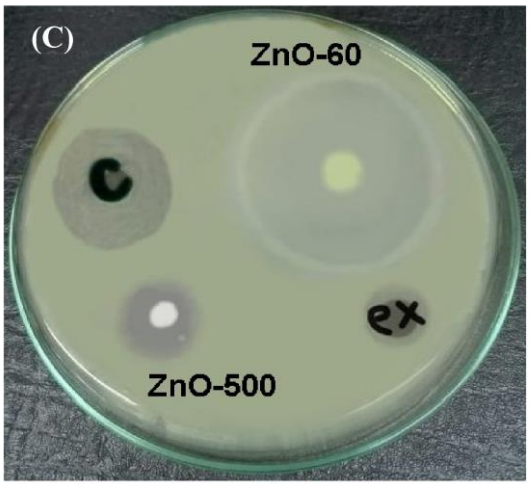

Figure 6. The antibacterial activity of the synthesized ZnO nanoparticles. **(a)** Inhibitory effect of the synthesized zinc oxide nanoparticles on *Helicobacter pylori* (ATCC 700392) and Methicillin-Resistant *Staphylococcus aureus* compared with standard antibiotics (Metronidazole and Norfloxacin, respectively) that were used as positive control (1000 µg/mL). The tested concentration from zinc nanoparticles was 2 and 10 mg/mL against *H. pylori* and MRSA, respectively. Results were shown as the mean inhibition zone diameter (mm) ± standard deviation of three independent experiments. **(b),** The minimum inhibitory concentration (MIC) values against *H. pylori* and MRSA. (c) Inhibition zone presented in (A) for MRSA**.**

3.6. Antioxidant activity

Antioxidant activity of the green synthesized ZnONps using *P. oleracea* aqueous extract was also evaluated using DPPH free radical scavenging assay with the results presented in Figure 7. Generally, the synthesized ZnONPs exhibited a concentration-dependent effect in DPPH free radical scavenging activity. The radical scavenging capacity of *P. oleracea* mediated synthesized ZnO-60 Nps slightly lower than ascorbic acid standard in all tested concentrations (Fig. 7), but much higher than the ZnO-500 with IC_{50} values of 7.6, 33.1, 201.7 µg/ ml for ascorbic acid, ZnO-60, and ZnO-500, respectively. The radical scavenging activity of the synthesized ZnO-60 Nps was higher than ZnO-500 and this may be due to the bio-organic layer containing phenolic compounds capped the ZnO-60 from the extract that decomposed upon annealing in ZnO-500. Suresh et al **[**63**]** also reported that synthesized ZnONPs using *Cassia fistula* extract to exhibit significant antioxidant activities by scavenging of DPPH radicals.

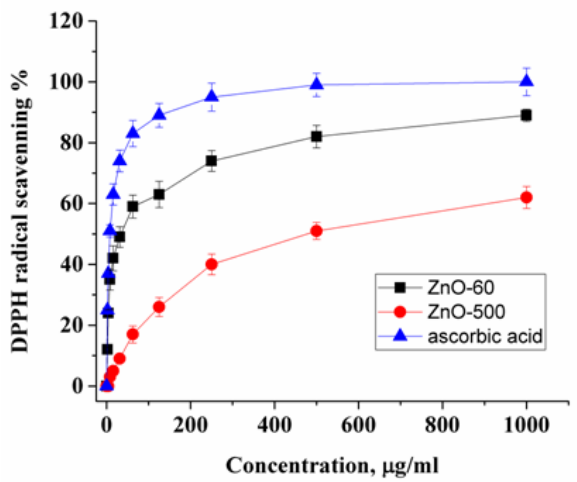

Figure 7. DPPH radical scavenging activity of the synthesized zinc nanoparticles compared with ascorbic acid as reference standard. Results were shown as the mean radical scavenging % ± SD of three independent experiments.

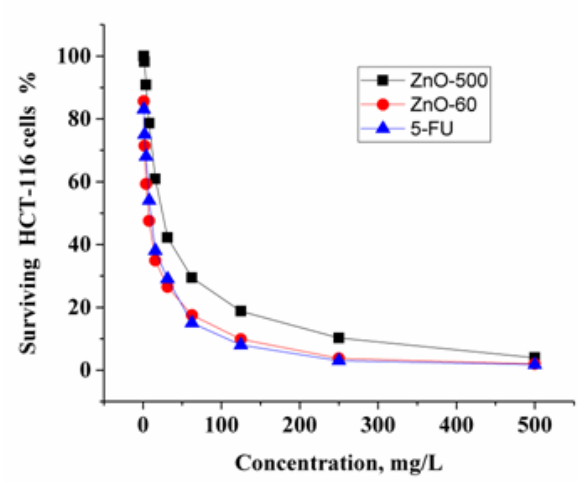

Figure 8: The dose response curve showing the *in vitro* inhibitory activity of the synthesized nanoparticles and 5-flourouracil reference standard against human colorectal carcinoma (HCT-116) cells after 48 h treatment using MTT assay..

3.7. Trypsin inhibition study

The enzymatic inhibitory activity of the synthesized zinc nanoparticles towards trypsin was also evaluated to explore the possible antiinflamatory role of the synthesized zinc nanoparticles. The results showed that among the tested Zn nanoparticles submitted to the screening test, ZnO-60 showed the highest enzyme inhibition (23.8%) compared to ZnO-500 (5.3%).

3.8. In vitro cytotoxic activity

The synthesized zinc nanoparticles were screened for cytotoxic activity (using MTT viability assay) against colon adenocarcinoma cell line HCT-116 compared with 5-fluorouracil standard drug. The plot showing the dose-response curves was presented in Fig. 8 of which the concentration required to inhibit 50% of the carcinoma cells (IC_{50}) was calculated. Many previous reports suggesting the green synthesis of ZnONPs using various medicinal plants has been reported to exhibit cytotoxic activities including the following plants *Costus pictus* [**64**], *Pongamia pinnata* [**65**], *Vitex negundo* [**66**] and *Cassia auriculata* [**67**].

The results of this study showed that biologically synthesized ZnONPs significantly inhibited the survival of HCT-116 cells with increasing the tested concentration compared with untreated control (*P*,0.001, Figure 6. ZnO-60 nanoparticles showed higher inhibitory activities against human HCT-116 cell line (IC_{50} 24.7 ± 1.1µg/ml) compared with ZnO-500 (IC_{50} 103.5 ± 6.2µg/ml); (reference drug 5-FU (IC_{50} 10.2 µg/ml), (Fig. 8**).**

4.Conclusions

In this study, the biosynthesis of ZnONPs utilizing *Portulaca oleracea seeds* aqueous extract has been reported. The reported method is a green, plant-extract mediated and low-cost approach that is capable of synthesizing ZnONPs at pH 7 with heating at 60 ^{0}C for one hour. To demonstrate the efficiency of the capping bioorganic molecules on ZnO nanoparticles, a part of the product was dried at 60 ^{0}C and the other part was annealed at 500 ^{0}C. Both synthesized ZnONPs was crystalline in nature and hexagonal in shape with an average size of 14 nm and 34.5 nm for ZnO-60 and ZnO-500, respectively, as evidenced by XRD and TEM analysis. The synthesized nanoparticles showed high antioxidant, good antibacterial activity, which has inhibited the growth of *Helicobacter pylori* (ATCC 700392) and Methicillin-Resistant *Staphylococcus aureus* bacteria and anticancer activity for HCT-116 cells with a higher efficiency of ZnO-60 than ZnO-500.

5. Conflicts of interest

There are no conflicts to declare.

References

[1] D. Segets, J. Gradl, R.K. Taylor, V. Vassilev, W. Peukert, Analysis of Optical Absorbance Spectra for the Determination of ZnO Nanoparticle Size Distribution, Solubility, and Surface Energy, ACS

Nano. 3 (2009) 1703–1710. https://doi.org/10.1021/nn900223b

[2] P.K. , H. Mishra, A. Ekielski, S. Talegaonkar, B. Vaidya, Zinc oxide nanoparticles: a promising nanomaterial for biomedical applications, Drug Discovery Today. 22 (2017) 1825–1834. https://doi.org/10.1016/j.drudis.2017.08.006

[3] J.A. Ruszkiewicz, A. Pinkas, B. Ferrer, T.V. Peres, A. Tsatsakis, M. Aschner, Neurotoxic effect of active ingredients in sunscreen products, a contemporary review, Toxicology Reports. 4 (2017) 245–259. https://doi.org/10.1016/j.toxrep.2017.05.006

[4] S. Rahimi, S. Salarinasab, N. Ghasemi, R. Rahbarghazi, S. Shahi, A.S. Milani, et al., In vitro induction of odontogenic activity of human dental pulp stem cells by white Portland cement enriched with zirconium oxide and zinc oxide components, Journal of Dental Research, Dental Clinics, Dental Prospects. 13 (2019) 3–10. https://doi.org/10.15171/joddd.2019.001

[5] V. Consonni, J. Briscoe, E. Kärber, X. Li, T. Cossuet, ZnO nanowires for solar cells: a comprehensive review, Nanotechnology. 30 (2019) 362001. http://doi.org/10.1088/1361-6528/ab1f2e

[6] X. Bai, L. Li, H. Liu, L. Tan, T. Liu, X. Meng, Solvothermal Synthesis of ZnO Nanoparticles and Anti-Infection Application in Vivo, ACS Applied Materials & Interfaces. 7 (2015) 1308–1317. https://doi.org/10.1021/am507532p

[7] A. Naveed Ul Haq, A. Nadhman, Ikram Ullah, G. Mustafa, M. Yasinzai, I. Khan, Synthesis Approaches of Zinc Oxide Nanoparticles: The Dilemma of Ecotoxicity, Journal of Nanomaterials. 2017 (2017) 1–14. https://doi.org/10.1155/2017/8510342

[8] S. Ahmed, Annu, S.A. Chaudhry, S. Ikram, A review on biogenic synthesis of ZnO nanoparticles using plant extracts and microbes: A prospect towards green chemistry, Journal of Photochemistry and Photobiology B: Biology. 166 (2017) 272–284. https://doi.org/10.1016/j.jphotobiol.2016.12.011

[9] S.P. Chandran, M. Chaudhary, R. Pasricha, A. Ahmad, M. Sastry, Synthesis of Gold Nanotriangles and Silver Nanoparticles Using Aloe vera Plant Extract, Biotechnology Progress. 22 (2006) 577–583. https://doi.org/10.1021/bp0501423

[10] K. Ali, S. Dwivedi, A. Azam, Q. Saquib, M.S. Al-Said, A.A. Alkhedhairy, et al., Aloe vera extract functionalized zinc oxide nanoparticles as nanoantibiotics against multi-drug resistant clinical bacterial isolates, Journal of Colloid and Interface Science. 472 (2016) 145–156. https://doi.org/10.1016/j.jcis.2016.03.021

[11] J. Qu, X. Yuan, X. Wang, P. Shao, Zinc accumulation and synthesis of ZnO nanoparticles using Physalis alkekengi L., Environmental Pollution. 159 (2011) 1783–1788. https://doi.org/10.1016/j.envpol.2011.04.016

[12] R.S. Devi, R. Gayathri, Green Synthesis of Zinc Oxide Nanoparticles by using Hibiscus rosa-sinensis, International Journal of Current Engineering and Technology. 4 (2014) 2444–2446

[13] S.R. Senthilkumar, S. Thirumal, Green tea (*Camellia sinensis*) mediated synthesis of zinc oxide (ZnO) nanoparticles and studies on their antimicrobial activities, International Journal of Pharmacy and Pharmaceutical Sciences. 6 (2014) 461–465.

[14] R. Perveen, S. Shujaat, Z. Qureshi, S. Nawaz, M.I. Khan, M. Iqbal, Green versus sol-gel synthesis of ZnO nanoparticles and antimicrobial activity evaluation against panel of pathogens, Journal of Materials Research and Technology 9 (2020) 7817-7827. https://doi.org/10.1016/j.jmrt.2020.05.004

[15] S. Jafarirad, M. Mehrabi, B. Divband, M. Kosari-Nasab, Biofabrication of zinc oxide nanoparticles using fruit extract of Rosa canina and their toxic potential against bacteria: A mechanistic approach, Materials Science and Engineering: C. 59 (2016) 296–302. https://doi.org/10.1016/j.msec.2015.09.089

[16] H. Çolak, E. Karaköse, Green synthesis and characterization of nanostructured ZnO thin films using Citrus aurantifolia (lemon) peel extract by spin-coating method, Journal of Alloys and Compounds. 690 (2017) 658–662. https://doi.org/10.1016/j.jallcom.2016.08.090

[17] K. Xu, H. Yan, M. Cao, X. Shao, Selaginella convolute extract mediated synthesis of ZnO NPs for pain management in emerging nursing care, Journal of Photochemistry and Photobiology B: Biology. 202 (2020) 111700. https://doi.org/10.1016/j.jphotobiol.2019.111700

[18] Q. Tang, H. Xia, W. Liang, X. Huo, X. Wei, Synthesis and characterization of zinc oxide nanoparticles from Morus nigra and its anticancer activity of AGS gastric cancer cells, Journal of Photochemistry and Photobiology B: Biology.

202 (2020) 111698. https://doi.org/10.1016/j.jphotobiol.2019.111698

[19] V. Hoseinpour, M. Souri, N. Ghaemi, A. Shakeri, Optimization of green synthesis of ZnO nanoparticles by Dittrichia graveolens (L.) aqueous extract, Health Biotechnology and Biopharma. 1 (2017) 39–49

[20] J. Cheng, X. Wang, L. Qiu, Y. Li, N. Marraiki, A.M. Elgorban, et al., Green synthesized zinc oxide nanoparticles regulates the apoptotic expression in bone cancer cells MG-63 cells, Journal of Photochemistry and Photobiology B: Biology. 202 (2020) 111644. https://doi.org/10.1016/j.jphotobiol.2019.111644

[21] M. Daniel, Medicinal Plants Chemistry and Properties, science publisher, Enfield, NH, 2006

[22] M.Z. Cui, H. Liu, C.Y. Li, Changes of blood glucose in diabetic rats and the interventional effect of purslane, Chinese Journal of Clinical Rehabilitation. 9 (2005) 92–93

[23] A. Movahedian, A. Ghannadi, M. Vashirnia, Hypocholesterolemic Effects of Purslane Extract on Serum Lipids in Rabbits Fed with High Cholesterol Levels, International Journal of Pharmacology. 3 (2007) 285–289. https://doi.org/10.3923/ijp.2007.285.289

[24] M.-I.K. El-Sayed, Effects of Portulaca oleracea L. seeds in treatment of type-2 diabetes mellitus patients as adjunctive and alternative therapy, Journal of Ethnopharmacology. 137 (2011) 643–651. https://doi.org/10.1016/j.jep.2011.06.020

[25] Y.Y. Lim, E.P.L. Quah, Antioxidant properties of different cultivars of Portulaca oleracea, Food Chemistry. 103 (2007) 734–740. https://doi.org/10.1016/j.foodchem.2006.09.025

[26] Y.-H. Li, C.-Y. Lai, M.-C. Su, J.-C. Cheng, Y.-S. Chang, Antiviral activity of Portulaca oleracea L. against influenza A viruses, Journal of Ethnopharmacology. 241 (2019) 112013. https://doi.org/10.1016/j.jep.2019.112013

[27] A. Gunenc, O. Rowland, H. Xu, A. Marangoni, F. Hosseinian, Portulaca oleracea seeds as a novel source of alkylresorcinols and its phenolic profiles during germination, Lwt. 101 (2019) 246–250. https://doi.org/10.1016/j.lwt.2018.10.075

[28] A.I. Mohamed, A.S. Hussein, Chemical composition of purslane (Portulaca oleracea), Plant Foods for Human Nutrition. 45 (1994) 1–9. https://doi.org/10.1007/bf01091224

[29] S.A. Petropoulos, Â. Fernandes, D.A. Arampatzis, N.G. Tsiropoulos, J. Petrović, M. Soković, et al., Seed oil and seed oil byproducts of common purslane (Portulaca oleracea L.): A new insight to plant-based sources rich in omega-3 fatty acids, LWT. 123 (2020) 109099. https://doi.org/10.1016/j.lwt.2020.109099

[30] N. Culpeper, Culpeper's complete herbal: a book of natural remedies for ancient ills, Wordsworth Editions, Ware, 1995.

[31] H.M. Burkill, The useful plants of West tropical Africa, 3rd ed., vol 4, Royal botanic gardens, Kew, 1997

[32] K.N. Thakkar, S.S. Mhatre, R.Y. Parikh, Biological synthesis of metallic nanoparticles, Nanomedicine: Nanotechnology, Biology and Medicine. 6 (2010) 257–262. https://doi.org/10.1016/j.nano.2009.07.002

[33] S. Iravani, Green synthesis of metal nanoparticles using plants, Green Chemistry. 13 (2011) 2638–2650. https://doi.org/10.1039/c1gc15386b

[34] G.F. Brooks, K.C. Carroll, J.S. Butel, S.A. Morse, Jawetz, Melnick & Adelberg's medical microbiology, 24th ed., McGraw-Hill Medical, New York, 2007

[35] CLSI. Performance Standards for Antimicrobial Susceptibility Testing; Twenty-Second Informational Supplement. CLSI document M100-S22. Wayne, PA: Clinical and Laboratory Standards Institute; 2012

[36] M.M. Ghorab, M.S. Alsaid, M.S.A. El-Gaby, N.A. Safwat, M.M. Elaasser, A.M. Soliman, Biological evaluation of some new N -(2,6-dimethoxypyrimidinyl) thioureido benzenesulfonamide derivatives as potential antimicrobial and anticancer agents, European Journal of Medicinal Chemistry. 124 (2016) 299–310. https://doi.org/10.1016/j.ejmech.2016.08.060

[37] C.-H. Lai, S.-H. Fang, Y.K. Rao, M. Geethangili, C.-H. Tang, Y.-J. Lin, et al., Inhibition of Helicobacter pylori-induced inflammation in human gastric epithelial AGS cells by Phyllanthus urinaria extracts, Journal of Ethnopharmacology. 118 (2008) 522–526. https://doi.org/10.1016/j.jep.2008.05.022

[38] C.Y. Hachem, J.E. Clarridge, R. Reddy, R. Flamm, D.G. Evans, S. Tanaka, et al., Antimicrobial susceptibility testing of Helicobacter pylori comparison of E-test, broth microdilution, and disk diffusion for ampicillin, clarithromycin, and metronidazole, Diagnostic Microbiology and Infectious Disease. 24 (1996) 37–41. https://doi.org/10.1016/0732-8893(95)00252-9

[39] T. Mosmann, Rapid colorimetric assay for cellular growth and survival: Application to proliferation and cytotoxicity assays, Journal of Immunological Methods. 65 (1983) 55–63. https://doi.org/10.1016/0022-1759(83)90303-4

[40] S. Puvanendran, A. Wickramasinghe, D.N. Karunaratne, G. Carr, D.S.A. Wijesundara, R. Andersen, et al., Antioxidant Constituents fromXylopia championii., Pharmaceutical Biology. 46 (2008) 352–355. https://doi.org/10.1080/13880200801887989

[41] M.L. Kakade, J.J. Rackis, J.E. McGhee, G. Puski, Determination of trypsin inhibitor activity of soy products: a collaborative analysis of an improved procedure., Cereal Chemistry. 51 (1974) 376–382

[42] M. Fazlzadeh, R. Khosravi, A. Zarei, Green synthesis of zinc oxide nanoparticles using Peganum harmala seed extract, and loaded on Peganum harmala seed powdered activated carbon as new adsorbent for removal of Cr(VI) from aqueous solution, Ecological Engineering. 103 (2017) 180–190. https://doi.org/10.1016/j.ecoleng.2017.02.052

[43] N. Matinise, X.G. Fuku, K. Kaviyarasu, N. Mayedwa, M. Maaza, ZnO nanoparticles via Moringa oleifera green synthesis: Physical properties & mechanism of formation, Applied Surface Science. 406 (2017) 339–347. https://doi.org/10.1016/j.apsusc.2017.01.219

[44] G. Sangeetha, S. Rajeshwari, R. Venckatesh, Green synthesis of zinc oxide nanoparticles by aloe barbadensis miller leaf extract: Structure and optical properties, Materials Research Bulletin. 46 (2011) 2560–2566. https://doi.org/10.1016/j.materresbull.2011.07.046

[45] O.J. Nava, C.A. Soto-Robles, C.M. Gómez-Gutiérrez, A.R. Vilchis-Nestor, A. Castro-Beltrán, A. Olivas, et al., Fruit peel extract mediated green synthesis of zinc oxide nanoparticles, Journal of Molecular Structure. 1147 (2017) 1–6. https://doi.org/10.1016/j.molstruc.2017.06.078

[46] A.K. Singh, P. Pal, V. Gupta, T.P. Yadav, V. Gupta, S.P. Singh, Green synthesis, characterization and antimicrobial activity of zinc oxide quantum dots using *Eclipta alba*, Materials Chemistry and Physics. 203 (2018) 40–48. https://doi.org/10.1016/j.matchemphys.2017.09.049

[47] S. Ameen, M.S. akhtar, H.shik shin, Semiconducting Nanostructures and Nanocomposites for the Recognition of Toxic Chemicals (A Review), Oriental Journal Of Chemistry. 29 (2013) 837–860. https://doi.org/10.13005/ojc/290302

[48] R., R. Snyder, Introduction to X-ray powder diffractometry, John Wiley & Sons, New York, 1996

[49] J.V. Meshram, V.B. Koli, M.R. Phadatare, S.H. Pawar, Anti-microbial surfaces: An approach for deposition of ZnO nanoparticles on PVA-Gelatin composite film by screen printing technique, Materials Science and Engineering: C. 73 (2017) 257–266. https://doi.org/10.1016/j.msec.2016.12.043

[50] N.L. Gavade, A.N. Kadam, Y.B. Gaikwad, M.J. Dhanavade, K.M. Garadkar, Decoration of biogenic AgNPs on template free ZnO nanorods for sunlight driven photocatalytic detoxification of dyes and inhibition of bacteria, Journal of Materials Science: Materials in Electronics. 27 (2016) 11080–11091. https://doi.org/10.1007/s10854-016-5225-7

[51] R.M. Silverstein, F.X. Webster, Spectrometric identification of organic compounds, 6th ed., Wiley, New York, 1997

[52] S.A. Khan, F. Noreen, S. Kanwal, A. Iqbal, G. Hussain, Green synthesis of ZnO and Cu-doped ZnO nanoparticles from leaf extracts of *Abutilon indicum*, Clerodendrum infortunatum, Clerodendrum inerme and investigation of their biological and photocatalytic activities, Materials Science and Engineering: C. 82 (2018) 46–59. https://doi.org/10.1016/j.msec.2017.08.071

[53] A.K. Zak, M.E. Abrishami, W.H.A. Majid, R. Yousefi, S.M. Hosseini, Effects of annealing temperature on some structural and optical properties of ZnO nanoparticles prepared by a modified sol–gel combustion method, Ceramics International. 37 (2011) 393–398. https://doi.org/10.1016/j.ceramint.2010.08.017

[54] S. Bakkiyaraj, S. Pandiyaraj, Evaluation of potential antimicrobial activity of some medicinal plants against common food-borne pathogenic

microorganism., International Journal of Pharma and Bio Sciences. 2 (2011) 484–491. https://doi.org/10.22376/ijpbs

[55] M. Premanathan, K. Karthikeyan, K. Jeyasubramanian, G. Manivannan, Selective toxicity of ZnO nanoparticles toward Gram-positive bacteria and cancer cells by apoptosis through lipid peroxidation, Nanomedicine: Nanotechnology, Biology and Medicine. 7 (2011) 184–192. https://doi.org/10.1016/j.nano.2010.10.001

[56] Y. Zhang, T.R. Nayak, H. Hong, W. Cai, Biomedical Applications of Zinc Oxide Nanomaterials, Current Molecular Medicine. 13 (2013) 1633–1645. https://doi.org/10.2174/15665240136661311111 30058

[57] R.K. Dutta, B.P. Nenavathu, M.K. Gangishetty, A.V.R. Reddy, Studies on antibacterial activity of ZnO nanoparticles by ROS induced lipid peroxidation, Colloids and Surfaces B: Biointerfaces. 94 (2012) 143–150. https://doi.org/10.1016/j.colsurfb.2012.01.046

[58] M. Čáp, L. Váchová, Z. Palková, Reactive Oxygen Species in the Signaling and Adaptation of Multicellular Microbial Communities, Oxidative Medicine and Cellular Longevity. 2012 (2012) 1–13. https://doi.org/10.1155/2012/976753

[59] X.-F. Zhang, W. Shen, S. Gurunathan, Silver Nanoparticle-Mediated Cellular Responses in Various Cell Lines: An in Vitro Model, International Journal of Molecular Sciences. 17 (2016) 1603. https://doi.org/10.3390/ijms17101603

[60] N. von Moos, V.I. Slaveykova, Oxidative stress induced by inorganic nanoparticles in bacteria and aquatic microalgae – state of the art and knowledge gaps, Nanotoxicology. 8 (2013) 605–630. https://doi.org/10.3109/17435390.2013.809810

[61] M. Gambino, F. Cappitelli, Mini-review: Biofilm responses to oxidative stress, Biofouling. 32 (2016) 167–178. https://doi.org/10.1080/08927014.2015.1134515

[62] U. Kadiyala, E.S. Turali-Emre, J.H. Bahng, N.A. Kotov, J.S. Vanepps, Unexpected insights into antibacterial activity of zinc oxide nanoparticles against methicillin resistantStaphylococcus aureus(MRSA), Nanoscale. 10 (2018) 4927–4939. https://doi.org/10.1039/c7nr08499d

[63] D. Suresh, R.M. Shobharani, P.C. Nethravathi, M.A.P. Kumar, H. Nagabhushana, S.C. Sharma, Artocarpus gomezianus aided green synthesis of ZnO nanoparticles: Luminescence, photocatalytic and antioxidant properties, Spectrochimica Acta Part A: Molecular and Biomolecular Spectroscopy. 141 (2015) 128–134. https://doi.org/10.1016/j.saa.2015.01.048

[64] J. Suresh, G. Pradheesh, V. Alexramani, M. Sundrarajan, S.I. Hong, Green synthesis and characterization of zinc oxide nanoparticle using insulin plant (Costus pictus D. Don) and investigation of its antimicrobial as well as anticancer activities, Advances in Natural Sciences: Nanoscience and Nanotechnology. 9 (2018) 015008. http://doi.org/10.1088/2043-6254/aaa6f1

[65] M. Sundrarajan, S. Ambika, K. Bharathi, Plant-extract mediated synthesis of ZnO nanoparticles using *Pongamia pinnata* and their activity against pathogenic bacteria, Advanced Powder Technology. 26 (2015) 1294–1299. https://doi.org/10.1016/j.apt.2015.07.001

[66] S. Ambika, M. Sundrarajan, Antibacterial behaviour of *Vitex negundo* extract assisted ZnO nanoparticles against pathogenic bacteria, Journal of Photochemistry and Photobiology B: Biology. 146 (2015) 52–57. https://doi.org/10.1016/j.jphotobiol.2015.02.020

[67] H. Padalia, P. Moteriya, S. Chanda, Synergistic Antimicrobial and Cytotoxic Potential of Zinc Oxide Nanoparticles Synthesized Using Cassia auriculata Leaf Extract, BioNanoScience. 8 (2017) 196–206. https://doi.org/10.1007/s12668-017-0463-6